



Steady plumes produced by downwellings in Earth-like vigor spherical whole mantle convection models

J. Huw Davies

*School of Earth, Ocean and Planetary Sciences, Cardiff University, Main Building, Park Place, Cardiff CF10 3YE, UK
(huw@earth.cf.ac.uk)*

[1] If mantle thermal upwellings (plumes) are the cause of volcanic “hot spots,” then observations suggest that plumes are relatively fixed with nonuniform distribution and limited lifetimes. To date, fixity of upwellings has only been shown in models of convection at either low-vigor or with layering, though studies where the lower mantle has high viscosity do frequently show upwellings with much lower drift velocities than the surface velocity. Since more vigorous convection traditionally shows more time dependence, fixity of upwellings has not been expected for nonlayered convection at Earth-like vigor; rather, we might expect slow but increasing drift velocities. I have undertaken numerical models of whole mantle convection in three-dimensional spherical geometry at approaching Earth-like vigor. Surprisingly, these simulations show prominent steady, virtually fixed, plumes arising from self-organization controlled by the smaller but numerous cold downwellings. If downwelling (subduction) dominates Earth’s interior dynamics, then this work suggests that plume fixity need not require layering. The regular spacing and permanence of model upwellings contrast with observations of hot spots though. In these models, which do not simulate plates, the fixity and regular spacing result from the freedom of downwellings to occur everywhere except where plumes reach the surface. I suggest that on Earth this feedback is weakened by the presence of plates but that whole mantle thermal convection can still produce relatively fixed plumes, though we might expect them to be weaker, more mobile, and transient.

Components: 8390 words, 10 figures, 2 tables, 3 animations.

Keywords: mantle; plumes; upwelling; convection; hot spots; heat transfer.

Index Terms: 1038 Geochemistry: Mantle processes (3621); 3037 Marine Geology and Geophysics: Oceanic hotspots and intraplate volcanism; 8121 Tectonophysics: Dynamics: convection currents, and mantle plumes; 8130 Tectonophysics: Heat generation and transport; 8137 Tectonophysics: Hotspots, large igneous provinces, and flood basalt volcanism.

Received 7 June 2005; **Revised** 26 July 2005; **Accepted** 30 September 2005; **Published** 1 December 2005.

Davies, J. H. (2005), Steady plumes produced by downwellings in Earth-like vigor spherical whole mantle convection models, *Geochem. Geophys. Geosyst.*, 6, Q12001, doi:10.1029/2005GC001042.

1. Introduction

[2] The conceptual model that hot spots (localized, primarily intraplate, volcanic provinces or chains) were due to stationary melting sources in the upper mantle beneath moving plates [Wilson, 1963] was refined so that they resulted from cylindrical hot upwellings in the mantle, plumes [Morgan, 1972]. While this concept might not explain all such volcanic provinces [Anderson, 1996; Foulger and Natland, 2003; King and Ritsema, 2000; Turcotte

and Oxburgh, 1973] it is still the most used paradigm by Earth scientists to explain the linked continental flood basalts/oceanic plateaus and the related hot spot tracks [Richards *et al.*, 1989]. The existence of plumes has also received encouraging, though not definitive, support from improved seismic imaging [Montelli *et al.*, 2004; Rhodes and Davies, 2001].

[3] For the plume model to succeed it needs to dynamically predict relatively stationary plumes



[Duncan and Richards, 1991; Molnar and Stock, 1987; Tarduno and Gee, 1995] (<3 cm/yr) whose life span substantially exceeds a mantle transit-time. Laboratory and numerical models have been presented that lead to plume fixity. The laboratory models have required a layered system [Davaille, 1999; Davaille et al., 2002; Jellinek and Manga, 2002] to generate stationary plumes. Stationarity was also reproduced numerically in layered convection in spherical geometry [Oldham and Davies, 2004]. Plume fixity has also been produced in numerical whole mantle spherical convection models, but only at low to intermediate vigor [Bercovici et al., 1989; Bunge et al., 1997; Zhong et al., 2000]. Reduced plume mobility has also been observed in Cartesian models with significant bottom heating [Lowman et al., 2004], regional spherical models [Tan et al., 2002], and in some of the simulations run in 3D spherical geometry with increased viscosity in the lower mantle [Monnereau and Quéré, 2001; Zhong et al., 2000]. Many other models though show only ephemeral and/or mobile upwellings/plumes/thermals [Carrigan, 1985; Glatzmaier, 1988; Glatzmaier et al., 1990; Hansen and Ebel, 1988; Lithgow-Bertelloni et al., 2001; Malevsky et al., 1992; Sirovich et al., 1989; Yuen et al., 1993]. Since convective velocities in boundary layer theory of Rayleigh-Benard convection scales as the two-third power of the Rayleigh number [Turcotte and Oxburgh, 1967], one might expect plume fixity to be weaker as Rayleigh number and mantle velocities increase and approach Earth-like vigor. We show here, rather counter intuitively, that it is possible to generate very steady, permanent, plumes in whole mantle convection at Earth-like vigor in spherical geometry over the likely range of bottom heating.

[4] The highest vigor to date in 3D spherical geometry has probably been reached in the work of Monnereau and Quéré [2001], who investigated the influence of viscosity structure, level of basal heating and the presence of piecewise continuous plates of fixed geometry, using models with average 30 km vertical grid node spacing. The fixity and structure of upwellings was not the focus of their work, but in one simulation with a more viscous lower mantle and low basal heating there are only 3 upwellings, which we are told are only slowly drifting. Otherwise the highest vigor reached in 3D spherical geometry has had 200 km thick thermal lithospheres, and had plate motion history applied at the surface [Bunge and Davies, 2001; Bunge and Grand, 2000; Bunge et al., 1998, 2003; Davies and Bunge, 2001]. In these earlier models

the applied plate motion history has a strong influence on the downwelling structures, while the deep upwelling structures tend to sustain a polygonal cell form to very shallow depths in the mantle. The earliest simulations in 3D spherical geometry at low vigor were steady state and had simple steady tetrahedral or cubic patterns with cylindrical upwellings and sheet like downwellings that break up at depth [Bercovici et al., 1989], and similar features were present when the viscosity was made temperature dependent [Ratcliff et al., 1996]. A more recent work, at higher vigor, (~300 km thick lithospheres), with temperature dependent viscosity and incompressible flow again showed nonsteady cylindrical upwelling structures, and downwelling sheets [Zhong et al., 2000]. The evolution of the sheets and the length scale of the features depended upon the rheology, e.g., whether the viscosity was layered, whether plates were simulated or the degree of temperature dependence in the rheology [Monnereau and Quéré, 2001; Zhong et al., 2000]. There has been a vigorous debate as to whether hot spots are the result of mantle plumes, with many arguing for alternative explanations [Anderson, 2000; Foulger et al., 2001; King and Anderson, 1995; King and Ritsema, 2000; McDougall, 1971; Meibom et al., 2003; Ritsema and Allen, 2003; Smith and Lewis, 1999; Turcotte and Oxburgh, 1973]. It is clearly very important therefore to discover whether this planform of linear downwellings and cylindrical upwelling active features, still holds at Earth-like vigor. The presence of plumes in Earth-like models is a necessary, but of course not sufficient, condition for plumes to be the cause of some (or all) hot spots.

2. Convection Models

[5] The numerical benchmarked model TERRA, [Baumgardner, 1985; Baumgardner and Frederickson, 1985] was used to solve the infinite Prandtl number conservation of momentum equation, the compressible conservation of mass equation assuming a Murnaghan equation of state [Bunge et al., 1997], and the conservation of energy equation including thermal dissipation. The assumed equation of state leads to a coefficient of thermal expansion, which fits experimental observations [Chopelas and Boehler, 1992], monotonically decreasing with depth from $\sim 4 \times 10^{-5} \text{ K}^{-1}$ at the surface, to $\sim 1.25 \times 10^{-5} \text{ K}^{-1}$ at the Core Mantle Boundary (CMB), as illustrated in Figure 1.

[6] The runs presented here use approximately 80 million nodes, this leads to an average lateral

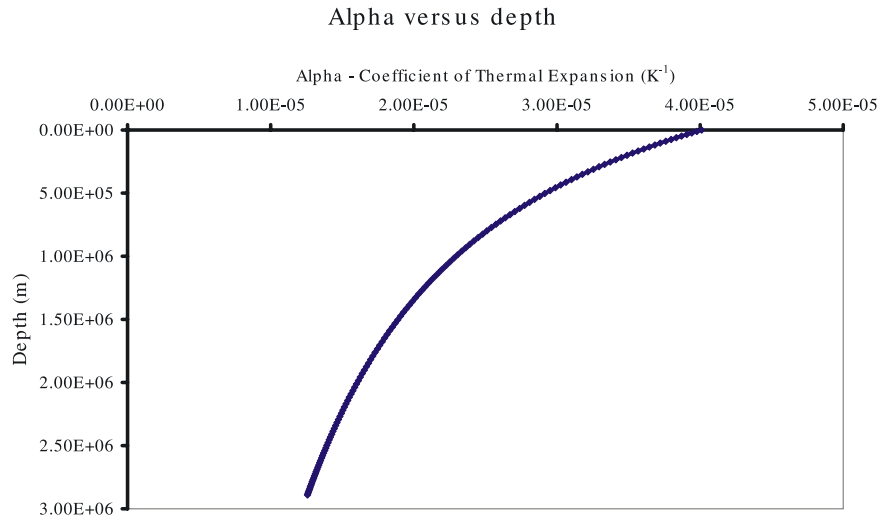


Figure 1. Variation of the coefficient of thermal expansion as a function of depth through the mantle. There is a decrease of ~ 3 through the depth of the mantle.

spacing in mid-mantle of around 22 km. The radial spacing is nonuniform with a reduced spacing in the boundary layers near the surface and the core mantle boundary, leading to 10 points in the upper 120 km. Given that the active features have a relatively large scale (minimum radius of the plumes is estimated at over 200 km, while the average thickness of the upper thermal boundary layer is around 95 km, bottom one even greater) we are confident that the calculations are fully resolved. The scale of the features is controlled by the viscosity which we set at 2×10^{21} Pa s. This choice allows us to be confident of both resolved calculations and near Earth-like vigor (of heat flow and surface velocity). These calculations easily surpass the rule-of-thumb of 5 points per high gradient region quoted by *Lowman et al.* [2004] and have at least an order of magnitude more nodes than the calculation of *Monnereau and Quéré* [2001], though their and our methods are not directly comparable. We cannot demonstrate categorically that the runs do not suffer from under-resolution since we do not have the computational resources to repeat the calculation at the next highest resolution (a calculation requiring ~ 500 GB RAM). We note that the movies can hint at under-resolution but these are artifacts of the graphics which need to throw away every other point in each direction, i.e., an 8 fold reduction in data, to allow reasonable performance even on a large Beowulf cluster (128 processors).

[7] The other model parameters for the reference model (run 1) are presented in Table 1. The

viscosity of the lower mantle is 40 times greater than the upper mantle, with the viscosity of the upper mantle being 2×10^{21} Pas. The variation of viscosity with depth is shown in Figure 2. The model has an approximately chondritic rate of internal heating, but with a depth varying heat generation which mimics the *Bercovici and Karato* [2003] model (Figure 3). The rate of internal heat generation is 5×10^{-12} W kg⁻¹ in the lower mantle and transition zone (close to chondritic estimates) [*Davies, 1999*]. This increases to 5×10^{-11} W kg⁻¹ between 414 km and 393 km depth (this is meant to approximate the possible 20 fold increase in rate of heat generation suggested by their model over a 10 km thick zone; by a 10 fold increase over a 21 km thick zone), and then is 5×10^{-13} W kg⁻¹ in the shallowest mantle (similar to values estimated from the concentrations found in MORB with reasonable estimates of partition coefficients and degree of melting) [*Jochum et al., 1983*]. A model (run 5) with constant heat generation with depth was also run, and the character of the result was identical to the depth dependent heat generation rate showing that its details are not significant for the issues discussed here. This lack of influence of the distribution of heating with depth on convection has also been found by *Leahy and Bercovici* [2004]. The upper and lower velocity boundary conditions are free-slip to mimic the liquid core and the mobile surface with its plate tectonics. Similar simulations have been undertaken but using plate motion histories for the upper velocity boundary conditions; these results are being prepared for presentation elsewhere. The



Table 1. Parameters of Reference Model (Run 1)

Parameter	Value	Units
Upper mantle viscosity	2×10^{21}	Pa s
Lower mantle viscosity	8×10^{22}	Pa s
Thermal conductivity	5.5	$\text{W m}^{-1} \text{K}^{-1}$
Specific heat at constant pressure	1.15×10^3	$\text{J kg}^{-1} \text{K}^{-1}$
Surface temperature	300	K
Core mantle boundary temperature	2850	K
Acceleration due to gravity	10	ms^{-2}
Reference heat generation (lower mantle)	5×10^{-12}	W kg^{-1}
Model Clapeyron slope (410 km)	0.0	MPa K^{-1}
Model Clapeyron slope (660 km)	0.0	MPa K^{-1}
Murnaghan equations of state	See <i>Bunge et al.</i> [1997]	
Initial condition	small-scale random features	

initial thermal state of the model was one of very small random thermal perturbations at the nodes (i.e., very small length scale).

[8] To check the robustness of the results we have run a range of other models. The changes in the parameters from the reference case, for these additional cases are listed in Table 2. These include a hotter CMB (run 2), an insulating CMB (run 3), a large-scale initial condition (run 4), a model with uniform internal heating with depth (run 5), and a model with phase changes at 410 km and 660 km depth (run 5).

3. Results

[9] The primary result of these simulations is that we obtain a small number ($\sim 8-10$) of virtually fixed plumes, produced by the action of smaller (but much more numerous) cold downwelling structures. Once formed, following the initial transient, these plumes typically survive the remaining

length of the simulation (which approaches 2 Gyr, with the longest simulations approaching 3 Gyr in total).

[10] One might expect strong independent upwellings to be favored by a strong lower thermal boundary layer arising from high bottom heating. This work reports the results for a range of bottom heating that likely straddle Earth levels. For example, by the end of the reference model simulation (run 1, CMB temperature 2850 K) approximately 13 TW of heat enters the mantle from the core, $\sim 22\%$ of the model surface heat flow. For run 2 (CMB temperature 3400 K), by the end of the simulation approximately 18 TW of heat enters the mantle from the core, $\sim 27\%$ of the model's surface heat flow. Since all these models evolve thermally, the ratio of bottom heating to surface heat flow varies during the simulation and probably straddles Earth values during both model runs. The time dependence of the thermal evolution of these two models is presented in Figure 4 and Figure 5 (run 1

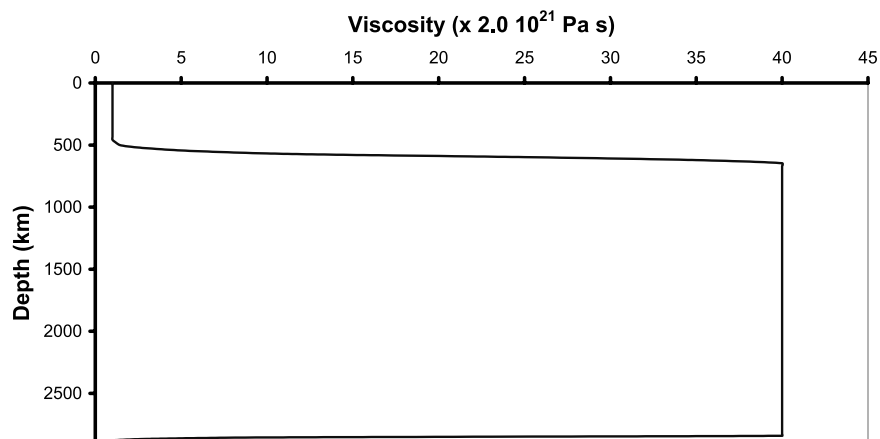


Figure 2. Variation of viscosity as a function of depth through the mantle. The lower mantle has viscosity a factor of 40 greater than the upper mantle viscosity.

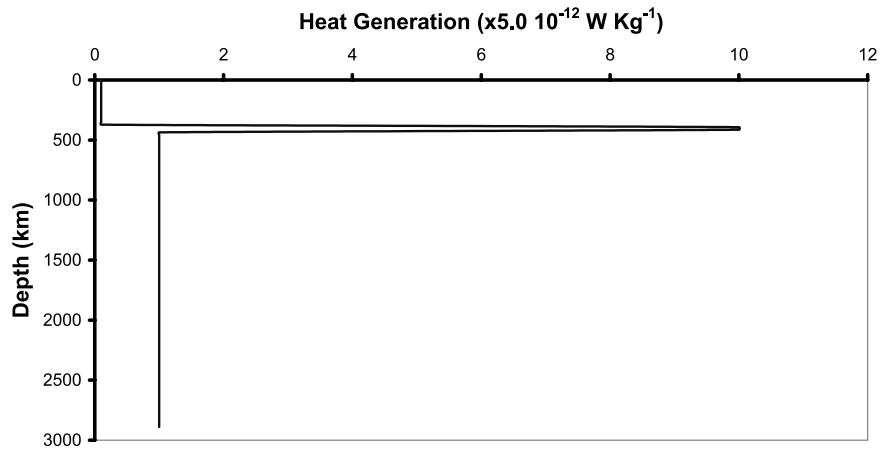


Figure 3. Variation of rate of internal heating as a function of depth through the mantle. This distribution attempts to crudely mimic the suggestion of *Bercovici and Karato* [2003]. Runs are also undertaken with constant rate of internal heating with depth, showing virtually identical results, e.g., run 5 presented in Figure 8.

and run 2, respectively). From these figures we note that after the initial transient the core heat flow varies from around 0–5% to the maximum percentage (22/27%) of surface heat flow by the end of the model runs. Plumes appear from more or less the start, when the CMB contribution is less than 10%. We have also run a model with a thermally insulated lower boundary (run 3), i.e., a case with no bottom heating. Even in this case we found, surprisingly, that we still got plume like features, though much weaker, provided there is sufficient internal heating for the downwellings to push down into polygonal structures and plumes. This all suggests that the exact value of the degree of bottom heating is not critical for this behavior. For comparison estimates for Earth’s present-day core heat flux range from around 2–3 TW [*Davies, 1988a; Sleep, 1990*] (5–8% of mantle heat flux (~37 TW)), through 6–12 TW (16–32%) [*Buffett, 2002*], to 13.4 TW (36%) [*Malamud and Turcotte, 1999*]. Estimates of the CMB temperature at 4000 ± 600 K [*Boehler, 1996*], are closer to run 2 than run 1. Very high CMB temperatures are not favored though in these models since they would produce even higher core heat flux. If the difference is related to too low an adiabatic temperature

drop being included in these models, then since the adiabatic temperature drop does not contribute to the dynamics, our conclusions should not be affected.

[11] As can be seen from Figures 4 and 5 the models clearly start hot and cool with time. As a result some of the surface heat flux is provided by the cooling, like on Earth; but in contrast to the Earth we neither let the core cool, nor have higher radioactivity in the past. Therefore the model is neither a traditional quasi-equilibrium model, nor is it a proper secular evolution model. With this set-up though we are able to incorporate secular cooling and get reasonable proportions of the various inputs to the mantle’s heat budget. Since we do not have temperature dependent viscosity it is probable that the time evolution of the cooling is not quite Earth-like and the model is possibly slightly “hot.” Since (once the transient is over) the plumes remain so fixed and constant throughout, even though the proportions and values of the various heat sources are changing dramatically, and there are no temperature dependent parameters, it is very unlikely that this evolution will affect the conclusions.

Table 2. Changed Model Parameters From Reference Model (Run 1) for Other Models

Model Run	Change	Value	Units
2	core mantle boundary temperature	3400	K
3	core mantle boundary temperature	insulating	
4	initial condition: large-scale spherical harmonic; degree 4 cubic; $P(l,m,\varphi)$	$P(4,0,0) + P(4,4,\pi/16)$	
5	uniform heating with depth	5×10^{-12}	$W \text{ kg}^{-1}$
6	model Clapeyron slope (410 km; 660 km)	1.75; -1.5	$MPa \text{ K}^{-1}$

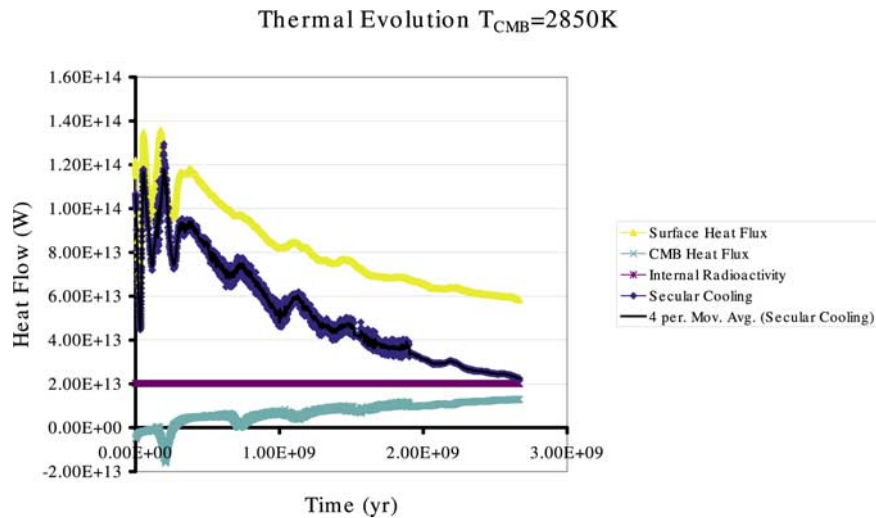


Figure 4. Thermal evolution of model run 1 ($T_{\text{CMB}} = 2850 \text{ K}$). The figures show how the surface heat flow, core mantle boundary heat flux, and the shell cooling (all in W) evolve with time (Gyr). For comparison we also show the level of radioactive heating which is constant with time. The brief period of negative core heat flux at the start of the simulation is an artifact arising in the early part of the unrealistic transient. At this time the mantle is virtually stationary and cannot lose its original heat or extra heat gained by internal and basal heating by inefficient thermal conductivity; hence it gets hotter than the core. The artifact rapidly disappears once the velocities increase as the convective instability grows.

[12] In Figures 6 and 7 we show the evolution of the root mean square (RMS) velocity of the whole mantle in the simulations. We see that the variations correlate closely with the temperature variations. We note that this average is around half the RMS surface velocity, which is 3.81 cm/yr at the end of run 1, and 4.20 cm/yr at the end of run 2. These surface velocities approach present-day RMS surface velocities of around 4.4 cm/yr.

[13] In Figure 8 we show a sequence of images (spaced 30 Myr apart) of the lateral temperature anomaly for run 1 (CMB temperature 2850 K), and in Figure 9 we show a very similar sequence for run 2 (CMB temperature 3400 K). In both cases we find that the downwellings ultimately reach the base of the mantle and push hot material down and away as they descend. One can see clearly how this process forces the hot mantle to collect in a cellular

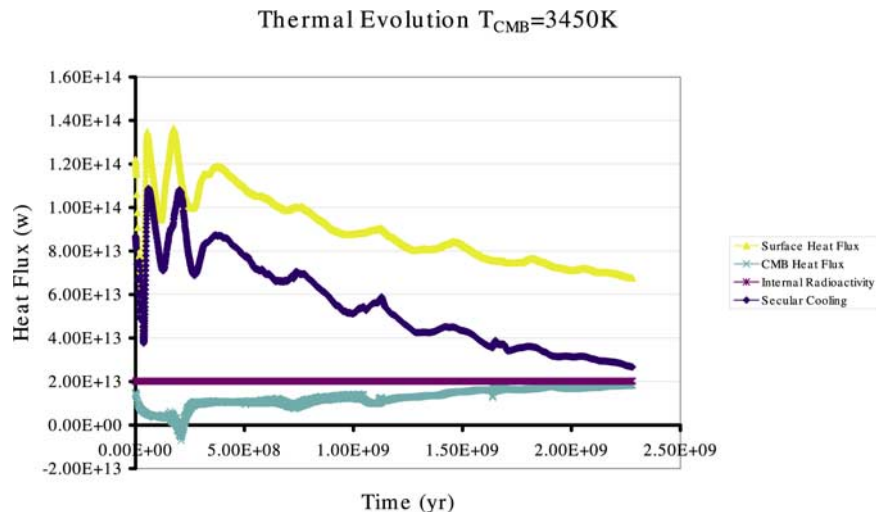


Figure 5. Thermal evolution of run 2 ($T_{\text{CMB}} = 3400 \text{ K}$). The figures show how the surface heat flow, core mantle boundary heat flux, and the shell cooling (all in W) evolve with time (Gyr). For comparison we also show the level of radioactive heating which is constant with time.

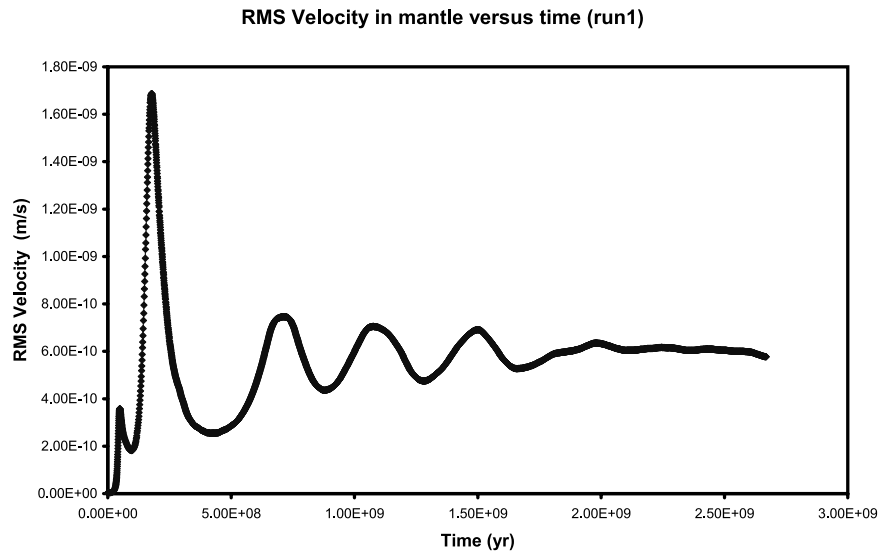


Figure 6. Evolution of velocity field in run 1 ($T_{\text{CMB}} = 2850$ K). The figure shows how the root mean square (RMS) velocity (m s^{-1}) throughout the whole model evolves with time (yr). We note that the RMS surface velocity is likely to be around a factor of 2 higher than the RMS of the whole flow. The RMS surface velocity is 3.8 cm/yr at the end of the simulation, while the RMS velocity of the whole field is around 1.9 cm/yr.

pattern at the CMB. In Figure 9 one can see how a line of hot material at the CMB (Figure 9b) is pushed downward and sideways (in Figures 9c, 9d, and 9e) by the increasing amount of cold (blue) material until it joins the hot ridge (in Figure 9f) already joining two prominent steady plumes. The return upward flow is focused at the junctions of the cellular pattern as strong steady cylindrical upwellings, which we will call plumes. The most

striking feature of the results as shown in these figures is that the plumes are very stationary and stable. These figures also show, though less clearly, that it is the downwellings that are controlling, even though they are less prominent.

[14] To illustrate how steady and stationary these plumes are, we have produced complete animations visualizing runs 1 and 2 (Animation 1, Animation 2).

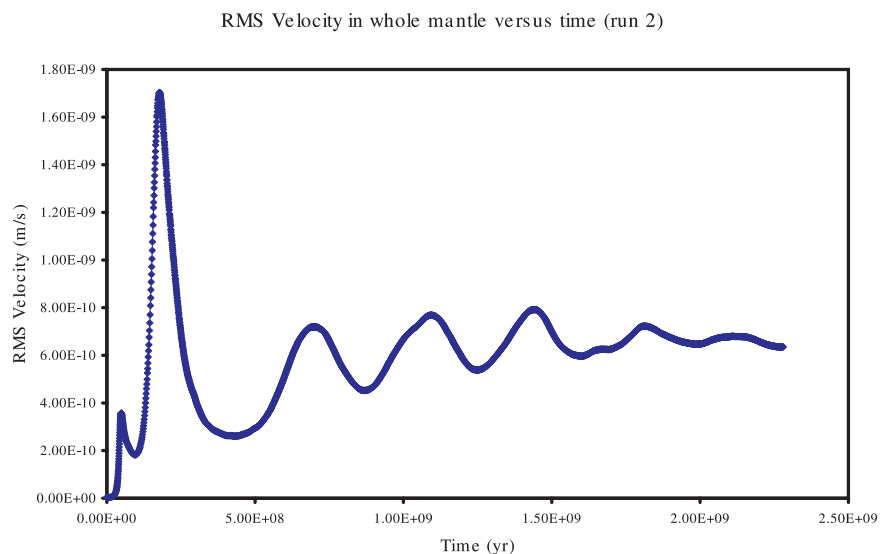


Figure 7. Evolution of velocity field of run 2 ($T_{\text{CMB}} = 3400$ K). The figure shows how the root mean square (RMS) velocity (m s^{-1}) throughout the whole model evolves with time (yr). We note that the RMS surface velocity is likely to be around a factor of 2 higher than the RMS of the whole flow. The RMS surface velocity is 4.2 cm/yr at the end of the simulation, while the RMS velocity of the whole mantle is around 2 cm/yr.

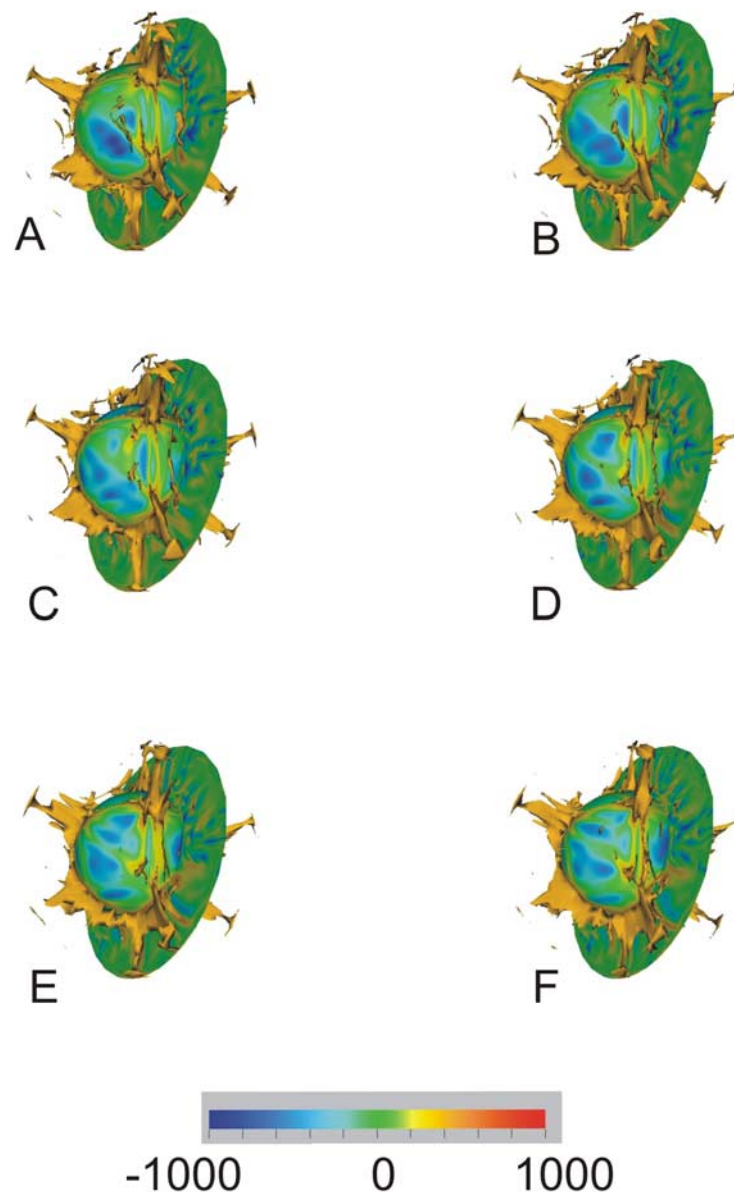


Figure 8. Time sequence of thermal structure of reference spherical whole mantle convection model. This figure shows a sequence of six snapshots of the thermal anomaly structure from run 1 (CMB 2850 K), spaced 30 Myr apart. Each snapshot shows a radial surface just above the core mantle boundary, a cross section, and a hot isosurface. The hot isosurface represents regions of the model which are 400 K hotter than the average for their depth. The scale shows what temperature away from the lateral average (thermal anomaly) the color represents. The most prominent features are the hot cylindrical plumes. They are also seen to be very robust and stable. The figure also illustrates how hot material, away from the plumes, moves down and sideways (this is driven by the cold downwellings, which we do not visualize in these figures for clarity, but can be appreciated somewhat from the cold (blue) regions on the CMB radial surface, but see Animation 3), such that it collects at ridges which are formed when hot material being brought together from two opposite directions meets. The plumes occur where the ridges meet. Since the simulations include compressibility, to better image the variation of the plume with depth, we should vary the isosurface value with depth to take account of the effect of compressibility [Albers and Christensen, 1996]. This minor adjustment is quite complicated to evaluate and implement, but since we do not try to quantify how the plumes vary in radius with depth, it is not important for our discussion.

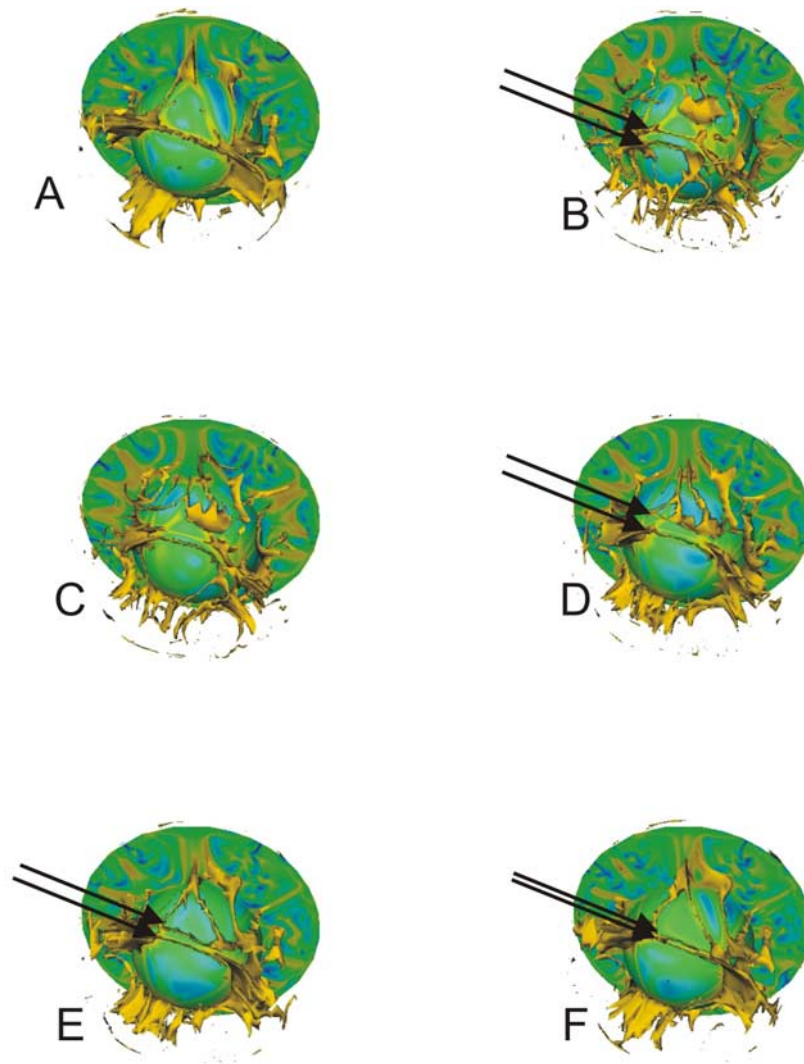
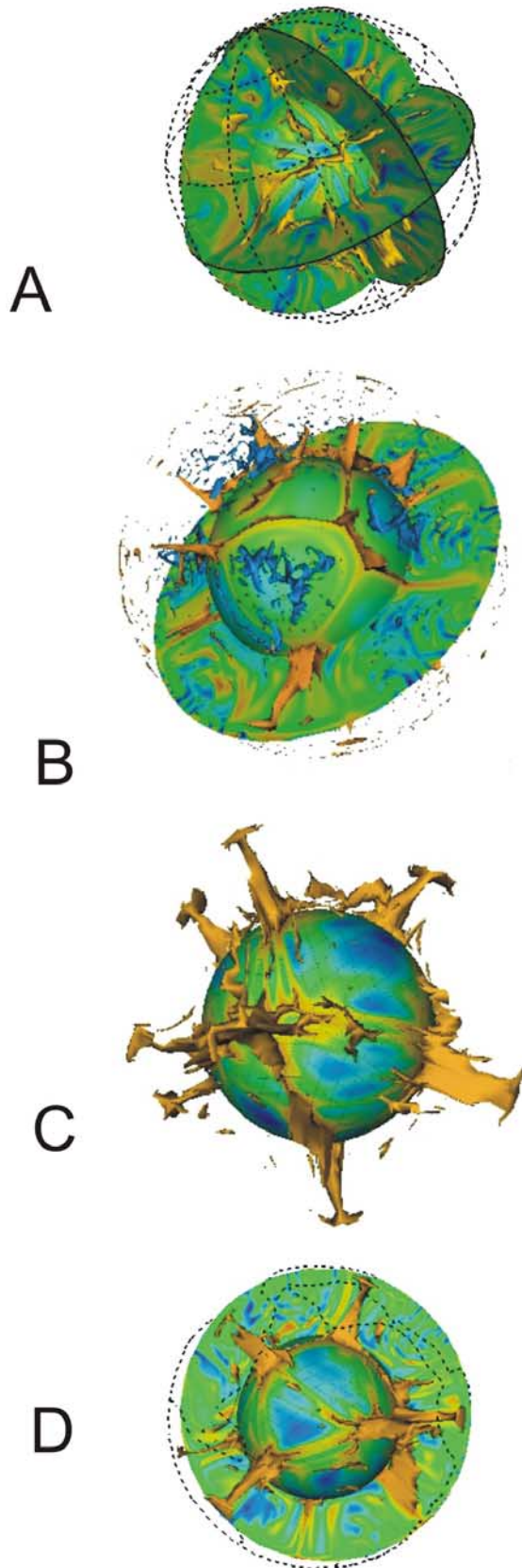


Figure 9. Time sequence of thermal structure of spherical whole mantle convection model with hotter Core Mantle Boundary. This figure is like Figure 8 but shows a sequence of six snapshots from run 2 (CMB 3400 K). The remarkable feature is again the prominent and stable upwellings, nearly identical to the plumes seen in Figure 8. This sequence shows even more clearly how this stable planform is generated by the collecting together of warm material by the downwelling material. We can see two lines of hot material being brought together to form a ridge at the CMB, from Figures 9b through to Figure 9e. These lines of hot material have been pointed out by black arrows.

These animations show a radial surface just above the CMB, and the isosurface for temperatures 400 K hotter than the lateral average. The color scheme for the animations is identical with the one for Figure 8, with blues representing colder than average temperatures, and yellows, orange and reds representing hotter than average temperatures. Both simulations have been run for over 2 Gyr. Given the RMS plate velocity of around 4cm/yr (again like the heat fluxes, very similar to Earth) this is around 24–28 mantle transit times ($2 \times 10^9 / (3 \times 10^6 / 0.04)$), or 6 to 7 overturn times for unit aspect ratio convection cells. The striking observation from these movies is that the plumes are prominent, steady and perma-

nent virtually throughout. In a third animation (Animation 3), we show again the results of run 1 but in addition to the hot isosurface we show a cold isosurface (500 K colder). This shows most clearly how the smaller, but numerous, downwellings, play a critical role in generating this very stable pattern.

[15] In Figure 10 we present snapshots from runs 3, 4, 5 and 6. We can see that in cases 4, 5 and 6 we still have a small number of strong plumes. Even in case 3, which has no heating from the CMB we still have a few, if much weaker, upwelling plumes. These additional runs show that the phenomenon of strong steady plumes is reasonably independent



of the exact degree of core heating, the distribution of internal heating, the form of the initial condition (the small scales develop into the large-scale pattern, while the very large scale heterogeneity also modifies itself to the large-scale pattern of the other simulations), or the presence of phase changes (the values assumed for the model Clapeyron slopes are assuming an olivine content of around 65% in the mantle, i.e., actual Clapeyron slopes are $\sim 50\%$ larger ($\sim 2.6 \text{ MPa K}^{-1}$, 410 km, -2.3 MPa K^{-1} , 660 km)). This work does not investigate the newly identified perovskite to post-perovskite phase change very close to the CMB [Murakami *et al.*, 2004]. Early work suggests that it will tend to produce slightly more, weaker and less stable plumes [Nakagawa and Tackley, 2004] but the controlling parameters are currently poorly known. The work also does not consider the effect of depth

Figure 10. Thermal structure of snapshots from different whole mantle convection models. The figures all show the thermal structure in the mantle at the end of the respective simulations. They all show a radial surface just above the CMB, a hot isosurface which maps out the 400 K thermal anomaly, and the color scale is that of Figure 8. (a) This figure is from run 3, which has an insulating CMB. One would not expect such a model to produce any plumes at all since it does not have a thermal boundary layer at its base. The downwellings, though, organize the internal heat to form a polygonal structure at the CMB, which leads to weak plumes at the intersections. We have added a second cross section to this figure, which allows one to see the multiple weak plumes, which have not quite been merged to produce the strong plumes of the other simulations. The figure is surrounded by a latitude/longitude grid to give the reader a sense of the volume of the mantle. (b) This is run 4 with a large-scale spherical harmonic pattern initial condition, a degree 4 cubic harmonic pattern made up of equal amounts of a degree 4 order 0 pattern, and a degree 4 order 4 pattern shifted by $\pi/16$ radians. Again the remarkable feature is how similar this figure looks to Figure 8, showing that the results are virtually independent of the initial condition. This figure again has a grid to give the reader a sense of the surface. (c) This is run 5, which has a uniform degree of heating with depth. The remarkable feature again is how similar this figure looks to Figure 8, showing that the strong steady plumes are not sensitive to the details of the distribution of heating with depth. (d) This is run 6, which included the dynamical effects of phase boundaries at 410 km and 660 km depth. Again, the results display strong steady plumes, showing that the results are not sensitive to the presence or absence of phase boundaries, at least at these depths (410, 660 km) and reasonable Clapeyron values (~ 2.6 and -2.3 MPa K^{-1} , assuming 65% olivine mantle).



dependence of thermal conductivity, though work to date suggest that it will tend to favor large steady plumes [Dubuffet et al., 1999; Hofmeister, 1999].

4. Discussion

[16] While these models are very realistic in many aspects, they are missing at least two critical aspects of Earth's mantle convection. Due to computational limitations the models presented here do not have temperature dependent viscosity. Also the model does not generate plates at the surface, or have continents. Given that earlier work suggests that these aspects (plates and temperature dependent viscosity) do not change the basic planform, i.e., linear downwellings and plume like upwellings [Lowman et al., 2001; Zhong et al., 2000], then it is possible that some of the characteristics of the simulations presented here are representative of the processes in Earth's mantle (McNamara, personal communication). One such characteristic might be downwellings dominating mantle dynamics. This has also been argued in earlier work in Cartesian geometry and lower vigor spherical geometry [Bunge et al., 1997; Davies, 1988b]. If correct, this would suggest that subducting slabs might be partly responsible for the limited mobility of plumes. For example on Earth subducting slabs could be moving broad hot-zones along the CMB, forming sharp variations in lateral seismic velocity as observed seismically [Ni et al., 2002; Thomas et al., 2002] and even forming super-swells [Davaille, 1999; Tackley, 2000; Thompson and Tackley, 1998]. It would imply that upwelling features would tend to only be found away from regions of the CMB that have recently suffered impacting of subducting slabs. It is argued that this is what is observed [Anderson, 1998; Chase, 1985; Richards and Engebretson, 1992]. The majority of hot spots (believed by many to be the surface manifestations of upwelling plumes) occur in regions of geoid high [Chase, 1979; Stefanick and Jurdy, 1984], and negative seismic velocity anomalies. The geoid high and negative seismic velocity anomalies have been argued to arise from regions of the mantle without recent subducted material.

[17] The plumes last throughout the whole simulation once formed and therefore, probably, have a longer life span than Earth's hot spots. Since very few plumes "die," virtually no new plumes are "born" either, and hence other than the initial transient, we do not observe transient plume heads, but rather permanent plume head like features.

While this is unlikely to fit observations on Earth, we note that a model for flood basalts has invoked stationary plume heads [White and McKenzie, 1989]. The number of plumes is $\sim 8-10$ in nearly all the simulations. Again, while this is much smaller than the number of hot spots in catalogues (Morgan [1972]: 19; Crough and Jurdy [1980]: 42; Wilson [1973]: 66; Vogt [1981]: 117) and possibly unlikely to fit observations on Earth, it is interesting that it might not be much greater than the number of plumes with deep roots as imaged seismically (~ 6) [Montelli et al., 2004], especially if plume clusters [Schubert et al., 2004] are related to single plumes in our simulations. Courtillot et al. [2003], has also argued that only a small number of hot spots (possibly as few as 6) are underlain by deep-rooted plumes; though we note with little overlap with the ~ 6 plumes named by Montelli et al. [2004]. In respects of plume numbers and fixity the models presented here have probably been too successful in generating too few plumes which are too steady. That is, we should now be asking not the historical question of whether plumes can be made sufficiently permanent and fixed but whether they can be made more mobile and ephemeral.

[18] While it is true that in these simulations the downwellings control, and push around the upwellings, as observed also by Tan et al. [2002], the upwellings due to their fixity also ultimately control the locations of downwellings. They do this by making regions where they impact the surface too hot to form downwellings. This self-organization makes the planform exceptionally stable and also allows the upwellings to become more robust. This level of feedback does not seem to occur on Earth today. We argue that this is a reflection that the upper surface has tectonic plates and therefore the upwellings cannot as directly control the locations of subduction. If plates were added to our simulations we would still expect the downwellings to control, but then the downwellings would be localized to the location of subduction zones, breaking the symmetry. Also, with plates, the upwellings would not be able to feed back as effectively hence the planform would not be as stable, and therefore the upwellings would again be weaker. Also we expect that plate tectonics with its irregular geometry, variable plate sizes, and variable velocities will further break the strong symmetry and feedback that leads to the very steady plumes, and hence might lead to more realistic plumes. The history of subduction is possibly sufficiently steady for downwellings to generate upwelling plumes



with a level of relative fixity as seen on Earth, as suggested recently in kinematic models [Steinberger *et al.*, 2004]. This suggestion awaits future demonstration and testing in dynamic spherical models, though it tends to be supported by work to date in 3D Cartesian geometry [Lowman *et al.*, 2004].

[19] The stationarity of these features depends upon the increased viscosity in the lower mantle in these simulations. This reduced mobility of upwellings in systems with increased viscosity in the lower mantle has been observed in many previous numerical studies [Bunge *et al.*, 1996; Hansen *et al.*, 1993; Lowman *et al.*, 2004; Zhang and Yuen, 1995]. Such an increase in viscosity is plausible, and has been argued for from many directions [Forte *et al.*, 2002; Hager *et al.*, 1985; Ranalli, 2001]. The fixity is also favored by the reduced coefficient of thermal expansion in the lower mantle [Hansen *et al.*, 1991]. It is partly because they do not model depth dependent properties that the laboratory modeling community has argued that thermo-chemical convection is required to produce fixity in upwellings.

[20] In discussing temperature dependent rheology we start by noting that since mantle convection potentially has nonlinear feedbacks we cannot be totally confident how its addition would change features. Traditionally it has been expected that hot thermal plumes will have lower viscosity and as a result will become thinner features than plumes simulated in constant viscosity simulations. This is because the lower viscosity leads to higher plume velocity and hence the same heat flux can be transported by a plume with smaller cross section. Korenaga [2005] though has argued that since Montelli *et al.* [2004] claim to image plumes in the deep lower mantle, this suggests that they must have a larger diameter than earlier modeling work suggested one should expect. He suggests that this is because the plumes and lower mantle are in the diffusion creep regime, and that the high temperatures have encouraged grain growth such that the resulting large grain sizes increase viscosity [Solomatov, 1996]. In addition to the uncertainty regarding the temperature dependence of viscosity, it is also very difficult to model large lateral viscosity variations robustly, with the best simulations to date in spherical geometry being at Rayleigh numbers a few orders of magnitude less than Earth's mantle [Zhong *et al.*, 2000]. Low viscosity thermal plumes develop large heads on initiation. No heads develop if the viscosity of the

plumes is higher than that of the surrounding material. Therefore while our simulations have not had initiation heads or very thin plumes; those might be additional characteristics we might expect in simulations with temperature dependent viscosity. Modeling and constraining the temperature dependence of mantle viscosity should be one focus of future work.

5. Conclusion

[21] While it has been shown that plume fixity can develop in layered systems [Davaille *et al.*, 2002; Jellinek and Manga, 2002; Le Bars and Davaille, 2002; Oldham and Davies, 2004], I show using whole mantle spherical compressible convection models that even at \sim Earth-like vigor it is possible to have stationary strong plumes in whole mantle convection; i.e., without layering.

Acknowledgments

[22] I would like to acknowledge Ian Thomas (Cardiff) and Andy Heath (Liverpool) for developing the software used to visualize the model output and J. R. Baumgardner, H. P. Bunge, and colleagues, who have developed TERRA. I gratefully acknowledge the inputs provided by A. McNamara, two other anonymous reviewers, and P. van Keken (Editor), which improved the presentation and discussion. The computations were undertaken on Helix at Cardiff University, funded by SRIF (HEFCW), and NESSC at Liverpool University, funded by JREI (HEFCE).

References

- Albers, M., and U. R. Christensen (1996), The excess temperature of plumes rising from the core-mantle boundary, *Geophys. Res. Lett.*, *23*, 3567–3570.
- Anderson, D. L. (1996), The edges of the mantle, in *The Core-Mantle Boundary Region, Geodyn. Ser.*, vol. 28, edited by M. Gurnis *et al.*, pp. 255–271, AGU, Washington, D. C.
- Anderson, D. L. (1998), The scales of mantle convection, *Tectonophysics*, *284*, 1–17.
- Anderson, D. L. (2000), The thermal state of the upper mantle: No role for mantle plumes, *Geophys. Res. Lett.*, *27*, 3623–3626.
- Baumgardner, J. R. (1985), Three dimensional treatment of convective flow in the Earth's mantle, *J. Stat. Phys.*, *39*, 501–511.
- Baumgardner, J. R., and P. O. Frederickson (1985), Icosahedral discretization of the two-sphere, *SIAM J. Numer. Anal.*, *22*, 1107–1115.
- Bercovici, D., and S. Karato (2003), Whole-mantle convection and the transition-zone water filter, *Nature*, *425*, 39–44.
- Bercovici, D., G. Schubert, and G. A. Glatzmaier (1989), 3-dimensional spherical models of convection in the Earth's mantle, *Science*, *244*, 950–955.
- Boehler, R. (1996), Melting temperature of the Earth's mantle and core: Earth's thermal structure, *Annu. Rev. Earth Planet. Sci.*, *24*, 15–40.



- Buffett, B. A. (2002), Estimates of heat flow in the deep mantle based on the power requirements for the geodynamo, *Geophys. Res. Lett.*, *29*(12), 1566, doi:10.1029/2001GL014649.
- Bunge, H. P., and J. H. Davies (2001), Tomographic images of a mantle circulation model, *Geophys. Res. Lett.*, *28*, 77–80.
- Bunge, H. P., and S. P. Grand (2000), Mesozoic plate-motion history below the northeast Pacific Ocean from seismic images of the subducted Farallon slab, *Nature*, *405*, 337–340.
- Bunge, H.-P., M. A. Richards, and J. R. Baumgardner (1996), The effect of depth dependent viscosity on the planform of mantle convection, *Nature*, *379*, 436–438.
- Bunge, H. P., M. A. Richards, and J. R. Baumgardner (1997), A sensitivity study of three-dimensional spherical mantle convection at 10(8) Rayleigh number: Effects of depth-dependent viscosity, heating mode, and an endothermic phase change, *J. Geophys. Res.*, *102*, 11,991–12,007.
- Bunge, H.-P., M. A. Richards, C. Lithgow-Bertelloni, J. R. Baumgardner, S. Grand, and B. Romanowicz (1998), Time scales and heterogeneous structure in geodynamic earth models, *Science*, *280*, 91–95.
- Bunge, H. P., C. R. Hagelberg, and B. J. Travis (2003), Mantle circulation models with variational data assimilation: Inferring past mantle flow and structure from plate motion histories and seismic tomography, *Geophys. J. Int.*, *152*, 280–301.
- Carrigan, C. R. (1985), Convection in an internally heated, high Prandtl number fluid—A laboratory study, *Geophys. Astrophys. Fluid Dyn.*, *32*, 1–21.
- Chase, C. G. (1979), Subduction, the geoid, and lower mantle convection, *Nature*, *282*, 464–468.
- Chase, C. G. (1985), The geological significance of the geoid, *Annu. Rev. Earth Planet. Sci.*, *13*, 97–117.
- Chopelas, A., and R. Boehler (1992), Thermal expansivity in the lower mantle, *Geophys. Res. Lett.*, *19*, 1983–1986.
- Courtillot, V., A. Davaille, J. Besse, and J. Stock (2003), Three distinct types of hotspots in the Earth's mantle, *Earth Planet. Sci. Lett.*, *205*, 295–308.
- Crough, S. T., and D. M. Jurdy (1980), Subducted lithosphere, hot-spots, and the geoid, *Earth Planet. Sci. Lett.*, *48*, 15–22.
- Davaille, A. (1999), Simultaneous generation of hotspots and superswells by convection in a heterogeneous planetary mantle, *Nature*, *402*, 756–760.
- Davaille, A., F. Girard, and M. Le Bars (2002), How to anchor hotspots in a convecting mantle?, *Earth Planet. Sci. Lett.*, *203*, 621–634.
- Davies, G. F. (1988a), Ocean bathymetry and mantle convection: 1. Large flow and hotspots, *J. Geophys. Res.*, *93*, 10,467–10,480.
- Davies, G. F. (1988b), Role of the lithosphere in mantle convection, *J. Geophys. Res.*, *93*, 10,451–10,466.
- Davies, G. F. (1999), *Dynamic Earth: Plates, Plumes and Mantle Convection*, 458 pp., Cambridge Univ. Press, New York.
- Davies, J. H., and H. P. Bunge (2001), Seismically “fast” geodynamic mantle models, *Geophys. Res. Lett.*, *28*, 73–76.
- Dubuffet, F., D. A. Yuen, and M. Rabinowicz (1999), Effects of a realistic mantle thermal conductivity on the patterns of 3-D convection, *Earth Planet. Sci. Lett.*, *171*, 401–409.
- Duncan, R. A., and M. A. Richards (1991), Hotspots, mantle plumes, flood basalts, and true polar wander, *Rev. Geophys.*, *29*, 31–50.
- Forté, A. M., J. X. Mitrovica, and A. Espeset (2002), Geodynamic and seismic constraints on the thermochemical structure and dynamics of convection in the deep mantle, *Philos. Trans. R. Soc. London, Ser. A*, *360*, 2521–2543.
- Foulger, G. R., and J. H. Natland (2003), Is “hotspot” volcanism a consequence of plate tectonics?, *Science*, *300*, 921–922.
- Foulger, G. R., et al. (2001), Seismic tomography shows that upwelling beneath Iceland is confined to the upper mantle, *Geophys. J. Int.*, *146*, 504–530.
- Glatzmaier, G. A. (1988), Numerical simulations of mantle convection: Time-dependent three-dimensional compressible spherical shell, *Geophys. Astrophys. Fluid Dyn.*, *43*, 223–264.
- Glatzmaier, G. A., G. Schubert, and D. Bercovici (1990), Chaotic, subduction-like downflows in a spherical model of convection in the Earth's mantle, *Nature*, *347*, 274–277.
- Hager, B. H., R. W. Clayton, M. A. Richards, R. P. Comer, and A. M. Dziewonski (1985), Lower mantle heterogeneity, dynamic topography and the geoid, *Nature*, *313*, 541–545.
- Hansen, U., and A. Ebel (1988), Time-dependent thermal convection—A possible explanation for a multiscale flow in the Earth's mantle, *Geophys. J.*, *94*, 181–191.
- Hansen, U., D. A. Yuen, and S. E. Kroening (1991), Effects of depth-dependent thermal expansivity on mantle circulations and lateral thermal anomalies, *Geophys. Res. Lett.*, *18*, 1261–1264.
- Hansen, U., D. A. Yuen, S. E. Kroening, and T. B. Larsen (1993), Dynamic consequences of depth-dependent thermal expansivity and viscosity on mantle circulations and thermal structure, *Phys. Earth Planet. Inter.*, *77*, 205–223.
- Hofmeister, A. M. (1999), Mantle values of thermal conductivity and the geotherm from phonon lifetimes, *Science*, *283*, 1699–1706.
- Jellinek, A. M., and M. Manga (2002), The influence of a chemical boundary layer on the fixity, spacing and lifetime of mantle plumes, *Nature*, *418*, 760–763.
- Jochum, K. P., A. W. Hofmann, E. Ito, H. M. Seufert, and W. M. White (1983), K, U and Th in mid-ocean ridge basalt glasses and heat production, K/U and K/Rb in the mantle, *Nature*, *306*, 431–436.
- King, S. D., and D. L. Anderson (1995), An alternative mechanism of flood basalt formation, *Earth Planet. Sci. Lett.*, *136*, 269–279.
- King, S. D., and J. Ritsema (2000), African hot spot volcanism: Small-scale convection in the upper mantle beneath cratons, *Science*, *290*, 1137–1140.
- Korenaga, J. (2005), Firm mantle plumes and the nature of the core-mantle boundary region, *Earth Planet. Sci. Lett.*, *232*, 29–37.
- Le Bars, M., and A. Davaille (2002), Stability of thermal convection in two superimposed miscible viscous fluids, *J. Fluid Mech.*, *471*, 339–363.
- Leahy, G. M., and D. Bercovici (2004), The influence of the transition zone water filter on convective circulation in the mantle, *Geophys. Res. Lett.*, *31*, L23605, doi:10.1029/2004GL021206.
- Lithgow-Bertelloni, C., M. A. Richards, C. P. Conrad, and R. W. Griffiths (2001), Plume generation in natural thermal convection at high Rayleigh and Prandtl numbers, *J. Fluid Mech.*, *434*, 1–21.
- Lowman, J. P., S. D. King, and C. W. Gable (2001), The influence of tectonic plates on mantle convection patterns, temperature and heat flow, *Geophys. J. Int.*, *146*, 619–636.
- Lowman, J. P., S. D. King, and C. W. Gable (2004), Steady plumes in viscously stratified, vigorously convecting, three-dimensional numerical mantle convection models with mobile plates, *Geochem. Geophys. Geosyst.*, *5*, Q01L01, doi:10.1029/2003GC000583.



- Malamud, B. D., and D. L. Turcotte (1999), How many plumes are there?, *Earth Planet. Sci. Lett.*, *174*, 113–124.
- Malevsky, A. V., D. A. Yuen, and L. M. Weyer (1992), Viscosity and thermal fields associated with strongly chaotic non-Newtonian thermal convection, *Geophys. Res. Lett.*, *19*, 127–130.
- McDougall, L. (1971), Volcanic islands chains and sea floor spreading, *Nature*, *231*, 141–144.
- Meibom, A., D. L. Anderson, N. H. Sleep, R. Frei, C. P. Chamberlain, M. T. Hren, and J. L. Wooden (2003), Are high He-3/He-4 ratios in oceanic basalts an indicator of deep-mantle plume components?, *Earth Planet. Sci. Lett.*, *208*, 197–204.
- Molnar, P., and J. Stock (1987), Relative motions of hotspots in the Pacific, Atlantic and Indian Oceans since late Cretaceous time, *Nature*, *327*, 587–591.
- Monnerieu, M., and S. Quéré (2001), Spherical shell models of mantle convection with tectonic plates, *Earth Planet. Sci. Lett.*, *184*, 575–587.
- Montelli, R., G. Nolet, F. A. Dahlen, G. Masters, E. R. Engdahl, and S. H. Hung (2004), Finite-frequency tomography reveals a variety of plumes in the mantle, *Science*, *303*, 338–343.
- Morgan, W. J. (1972), Plate motions and deep mantle convection, *Mem. Geol. Soc. Am.*, *132*, 7–22.
- Murakami, M., K. Hirose, K. Kawamura, N. Sata, and Y. Ohishi (2004), Post-perovskite phase transition in MgSiO₃, *Science*, *304*, 855–858.
- Nakagawa, T., and P. J. Tackley (2004), Effects of a perovskite-post perovskite phase change near core-mantle boundary in compressible mantle convection, *Geophys. Res. Lett.*, *31*, L16611, doi:10.1029/2004GL020648.
- Ni, S. D., E. Tan, M. Gurnis, and D. Helmberger (2002), Sharp sides to the African superplume, *Science*, *296*, 1850–1852.
- Oldham, D., and J. H. Davies (2004), Numerical investigation of layered convection in a three-dimensional shell with application to planetary mantles, *Geochem. Geophys. Geosyst.*, *5*, Q12C04, doi:10.1029/2003GC000603.
- Ranalli, G. (2001), Mantle rheology: Radial and lateral viscosity variations inferred from microphysical creep laws, *J. Geodyn.*, *32*, 425–444.
- Ratcliff, J. T., G. Schubert, and A. Zebib (1996), Steady tetrahedral and cubic patterns of spherical shell convection with temperature-dependent viscosity, *J. Geophys. Res.*, *101*, 25,473–25,484.
- Rhodes, M., and J. H. Davies (2001), Tomographic imaging of multiple mantle plumes in the uppermost lower mantle, *Geophys. J. Int.*, *147*, 88–92.
- Richards, M. A., and D. C. Engebretson (1992), Large-scale mantle convection and the history of subduction, *Nature*, *355*, 437–440.
- Richards, M. A., R. A. Duncan, and V. E. Courtillot (1989), Flood basalts and hot-spot tracks—Plume heads and tails, *Science*, *246*, 103–107.
- Ritsema, J., and R. M. Allen (2003), The elusive mantle plume, *Earth Planet. Sci. Lett.*, *207*, 1–12.
- Schubert, G., G. Masters, P. Olson, and P. Tackley (2004), Superplumes or plume clusters?, *Phys. Earth Planet. Inter.*, *146*, 147–162.
- Sirovich, L., S. Balachandar, and M. R. Maxey (1989), Simulations of turbulent thermal convection, *Phys. Fluids A*, *1*, 1911–1914.
- Sleep, N. H. (1990), Hotspots and mantle plumes: Some phenomenology, *J. Geophys. Res.*, *95*, 6715–6736.
- Smith, A. D., and C. Lewis (1999), The planet beyond the plume hypothesis, *Earth Sci. Rev.*, *48*, 135–182.
- Solomatov, V. S. (1996), Can hotter mantle have a larger viscosity?, *Geophys. Res. Lett.*, *23*, 937–940.
- Stefanick, M., and D. M. Jurdy (1984), The distribution of hotspots, *J. Geophys. Res.*, *89*, 9919–9925.
- Steinberger, B., and R. Sutherland (2004), Prediction of Emperor-Hawaii seamount locations from a revised model of global plate motion and mantle flow, *Nature*, *430*, 167–173.
- Tackley, P. J. (2000), Mantle convection and plate tectonics: Toward an integrated physical and chemical theory, *Science*, *288*, 2002–2007.
- Tan, E., M. Gurnis, and L. Han (2002), Slabs in the lower mantle and their modulation of plume formation, *Geochem. Geophys. Geosyst.*, *3*(11), 1067, doi:10.1029/2001GC000238.
- Tarduno, J. A., and J. Gee (1995), Large-scale motion between Pacific and Atlantic hotspots, *Nature*, *378*, 477–480.
- Thomas, C., T. Heesom, and J. M. Kendall (2002), Investigating the heterogeneity of the D'' region beneath the northern Pacific using a seismic array, *J. Geophys. Res.*, *107*(B11), 2274, doi:10.1029/2000JB000021.
- Thompson, P. F., and P. J. Tackley (1998), Generation of megaplumes from the core-mantle boundary in a compressible mantle with temperature-dependent viscosity, *Geophys. Res. Lett.*, *25*, 1999–2002.
- Turcotte, D., and E. R. Oxburgh (1967), Finite amplitude convective cells and continental drift, *J. Fluid. Mech.*, *28*, 29–42.
- Turcotte, D. L., and E. R. Oxburgh (1973), Mid-plate tectonics, *Nature*, *244*, 337–339.
- Vogt, P. R. (1981), On the applicability of thermal conduction models to mid-plate volcanism: Comments, *J. Geophys. Res.*, *86*, 950–960.
- White, R., and D. McKenzie (1989), Magmatism at rift zones: The generation of volcanic continental margins and flood basalts, *J. Geophys. Res.*, *94*, 7685–7729.
- Wilson, J. T. (1963), A plausible origin of the Hawaiian Islands?, *Can. J. Phys.*, *41*, 863–870.
- Wilson, J. T. (1973), Mantle plumes and plate motions, *Tectonophysics*, *19*, 149–164.
- Yuen, D. A., U. Hansen, W. Zhao, A. P. Vincent, and A. V. Malevsky (1993), Hard turbulent thermal convection and thermal evolution of the mantle, *J. Geophys. Res.*, *98*, 5355–5373.
- Zhang, S. X., and D. A. Yuen (1995), The influences of lower mantle viscosity stratification on 3D spherical-shell mantle convection, *Earth Planet. Sci. Lett.*, *132*, 157–166.
- Zhong, S. J., M. T. Zuber, L. Moresi, and M. Gurnis (2000), Role of temperature-dependent viscosity and surface plates in spherical shell models of mantle convection, *J. Geophys. Res.*, *105*, 11,063–11,082.